

Enhanced Electrochemical Reactivity at Electrolyte/electrode Interfaces of Solid Oxide Fuel Cells with Ag Grids

Mingi Choi, Sangyeon Hwang, Doyoung Byun, and Wonyoung Lee[†]

Department of Mechanical Engineering, Sungkyunkwan University, Suwon 16419, Korea

(Received August 3, 2015; Revised August 20, 2015; Accepted August 20, 2015)

ABSTRACT

The specific role of current collectors was investigated at the electrolyte/electrode interface of solid oxide fuel cells (SOFCs). Ag grids were fabricated as current collectors using electrohydrodynamic (EHD) jet printing for precise control of the grid geometry. The Ag grids reduced both the ohmic and polarization resistances as the pitch of the Ag grids decreased from 400 μm to 100 μm . The effective electron distribution along the Ag grids improved the charge transport and transfer at the interface, extending the active reaction sites. Our results demonstrate the applicability of EHD jet printing to the fabrication of efficient current collectors for performance enhancement of SOFCs.

Key words : Solid oxide fuel cell, Electrolyte/electrode interface, Current collection, EHD jet printing, Ag grid

1. Introduction

The solid oxide fuel cell (SOFC) is a promising energy conversion device because of its high energy efficiency and potential to bring together the development of thermal power plants and environmental friendliness.¹⁾ To be more attractive in wider applications, however, an efficient current collector should be developed because SOFC performance depends not only on unit cells but also on the contact resistance between interconnects (or current collectors) and the cathode layer or the anode layer.²⁻⁷⁾ Substantial loss due to lateral conduction and contact resistance can impose practical limitations on the scale up of unit cells to stack systems. Moreover, even for unit cell systems, the accurate assessment of electrochemical performance may not be possible without a moderate current collector. Therefore, many groups have investigated the correlation between the efficiency of a current collector and its electrochemical performance.²⁻⁸⁾ Jiang *et al.* and Noh *et al.* reported improved performance with increasing of the contact area between the current collector and the cathode layer.^{3,5)} Jiang *et al.* showed that uneven current distribution at the electrolyte/electrode interfaces increased ohmic and polarization losses.³⁾ Guillodo *et al.* showed that the materials and types of current collectors affected the electrochemical performance.⁴⁾ However, the specific role of current collectors in the electrochemical performance, as well as optimization of their structures, has not been systematically investigated yet.

Typically, applications of Pt or Ag paste and mesh are used to fabricate current collectors. However, these methods are inappropriate to precisely control the geometry of the current collectors. Furthermore, it is not possible to apply these methods at the electrolyte/electrode interface because the effective reaction area would be blocked. As an alternative method to enable the fabrication of current collectors at the electrolyte/electrode interfaces, Choi *et al.* deposited a porous Ag layer using DC sputtering.⁹⁾ However, precise control of the current collectors was still nearly impossible, and the deposited Ag layer lost its porosity at elevated temperatures with degradation of the electrochemical performance.

To achieve fabrication of current collectors at the electrolyte/electrode interface, along with high controllability of the geometry, we employed electrohydrodynamic (EHD) jet printing. Due to its high resolution printing and good repeatability, EHD jet printing has been widely used for the fabrication of transparent electrodes with metal grids.¹⁰⁾ EHD jet printing also possess high industrialization potential because of its fast and large-area production, making it a promising fabrication method for current collectors. Precise control of the geometry of the metal grid and of the amount of target material is relatively simple and straightforward.

In this study, we demonstrated the enhancing effects of Ag grids fabricated by EHD jet printing on the electrochemical performance at the electrolyte/electrode interface. To investigate the geometrical effects, the pitch of the Ag grids was varied from 100 μm to 400 μm , while the shape of each grid was maintained. The morphology of the Ag grids was examined using optical and electron microscopy; the electrochemical performance was evaluated by electrochemical impedance spectroscopy. We successfully enhanced the elec-

[†]Corresponding author : Wonyoung Lee
E-mail : leewy@skku.edu
Tel : +82-31-299-4848 Fax : +82-31-290-5889

trochemical performance and showed the possibility of EHD jet printing as a highly efficient fabrication method for current collectors.

2. Experimental Procedure

Figure 1 shows the schematics of the EHD jet printing process. The EHD process was performed using an EHD jet printing unit (NP-200, ENJET). For high resolution printing, the relative humidity and the temperature were maintained at 45 - 47% and 20 - 25°C, respectively. Ag grids were printed symmetrically on both sides of single crystal yttria-stabilized zirconia (YSZ, 500 μm , 8 mol%, MTI Korea), the most common material used for SOFC electrolytes. A voltage of 1.45 kV was used over the distance of 500 μm between the nozzle and the substrate. The flow rate in the syringe pump was maintained at 0.3 $\mu\text{l}/\text{min}$. The printing velocity was 500 mm/s. The pitch of the grid structure was controlled from 100 to 400 μm at a 100 μm interval.

Polyethyleneoxide (PEO, 1,300,000 MW, Sigma-Aldrich) was used to prepare the Ag inks. Water and ethanol (3:2 volume ratio) were mixed and 3 wt% of PEO was added. Polymer added solvent was stirred via magnetic stirrer. After stirring, 25 wt% of Ag nanoparticles (ENJET) were added and stirred until mixed completely.

After spinning on the YSZ substrate, pre-sintering was performed at 200°C for 2 h to remove polymer and solvents. $\text{Sm}_{0.5}\text{Sr}_{0.5}\text{CoO}_3$ (SSC, KCERACELL CO.) powder was mixed

with the binder (VEH, Fuel Cell Materials) and resulting mixture was symmetrically printed on the sintered YSZ substrate with a thickness of approximately 40 μm . After screen printing, cell was sintered at 800°C for 8 h to evaporate the binder and form the microstructure of the electrode.

Secondary electron microscopy (SEM, JSM7000F, JEOL) was used to investigate the microstructure and geometry of the Ag grids and the SSC cathode layer. Electrochemical impedance spectroscopy (EIS) measurements were taken using the custom-made probe station in ambient air with an analyzing tool (GAMRY Reference 600, GAMRY INC.) in a frequency range from 0.01 Hz to 10⁶ Hz.

3. Results and Discussion

Figure 2 provides SEM images of the sintered Ag grids on the YSZ substrates with different pitches. The pitch between the Ag line patterns was changed to 100 μm (P100), 200 μm (P200), and 400 μm (P400). Each Ag line pattern formed a continuous dense structure with a width of 0.7 μm and height of 0.5 μm . No noticeable geometrical variation along the lines was observed. Some Ag particles were unexpectedly sputtered on the substrates because the jet flow was sensitive to unwanted changes of environment during printing. The influence of these particles, however, on the electrochemical performance can be considered to be negligible because of their marginal amount.

Figure 3 provides cross-sectional images of the samples with and without Ag grids between the YSZ electrolyte and the SSC cathode layer. Two samples exhibited identical microstructures with a thickness of 38 \pm 1 μm , showing that deposition of the cathode layer was not affected by the Ag grids underneath. Since the thickness of the Ag grids was about 500 nm, it was difficult to observe the Ag grids in the cross-sectional images.

Figure 4 shows the results of the EIS measurements in ambient air at 650°C from samples with no Ag grids (SSC only) and with Ag grids with pitches of 100 μm (P100), 200 μm (P200), and 400 μm (P400). With the Ag grids, both the ohmic and polarization resistances substantially decreased, as shown in Fig. 4(a). More interestingly, both the ohmic and the polarization resistance decreased with the decrease in pitch. Fig. 4(b) shows the area-specific resistance (ASR) values of the measured samples; there is a clear trend in

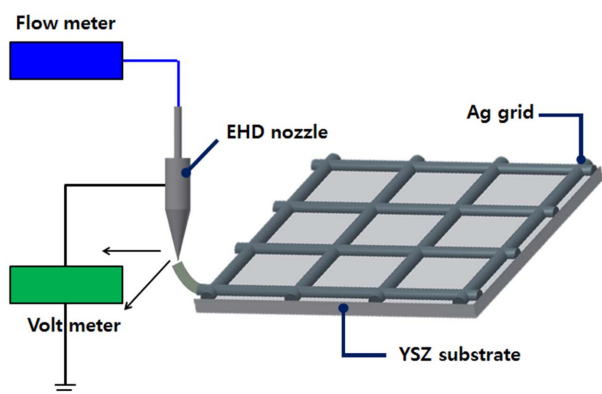


Fig. 1. Schematic of EHD jet printing process.

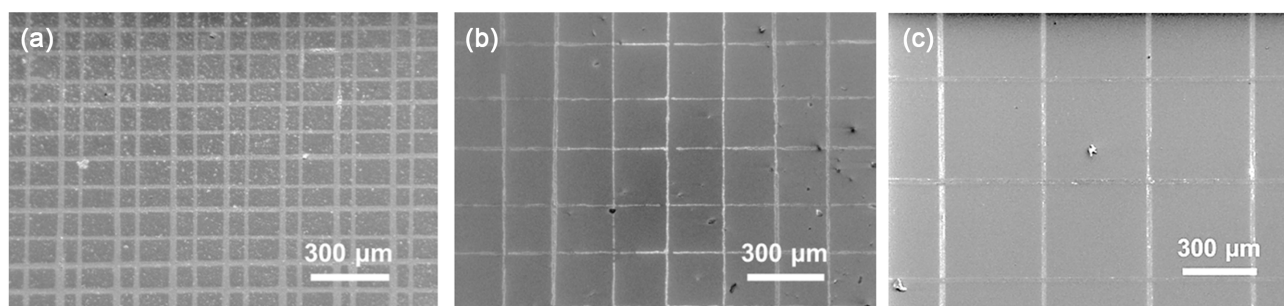


Fig. 2. SEM images of the Ag grids on the YSZ substrates with pitches of (a) 100 μm , (b) 200 μm , and (c) 400 μm .

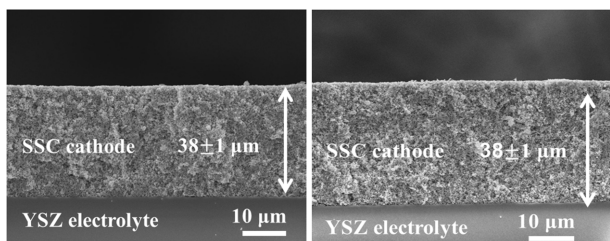


Fig. 3. Cross-sectional images of samples (a) without Ag grids, and (b) with Ag grids.

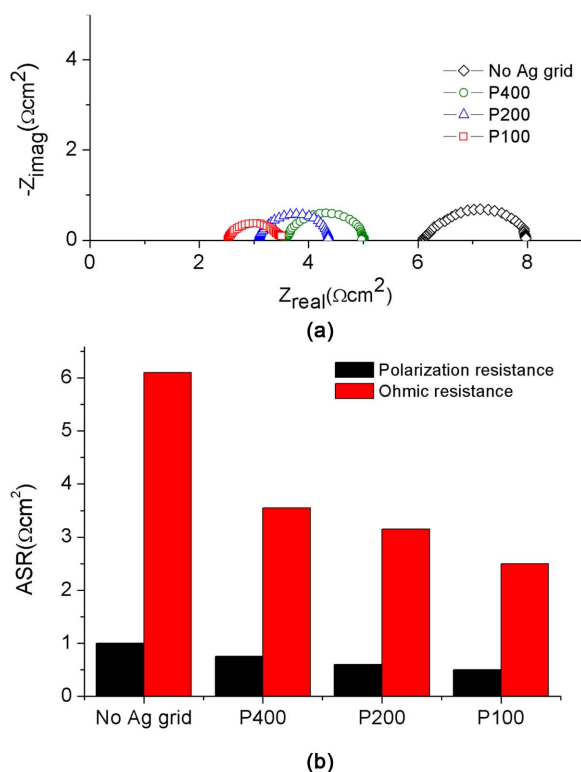


Fig. 4. (a) Nyquist plot of no Ag grids (black diamond), P400 (green circle), P200 (blue triangle), and P100 (red square). (b) Measured ASR of 4 samples. EIS measurements were performed in ambient air at 650°C.

which both resistances decreased with the Ag grids and the pitch. For example, the P100 sample exhibited approximately 2 times lower ohmic and polarization resistance values compared to the sample with no Ag grids. The measured ASR values are listed in Table 1.

Figure 5 shows the Arrhenius plot of the ohmic ASR of the sample with no Ag grids, P100, and the theoretical conductivity values of the single crystal YSZ.¹¹⁾ The slope represents the activation energy of oxygen ion diffusion. All samples showed almost identical activation energies, in a range of 1.07–1.09 eV, confirming that the diffusion mechanism remained the same and was not influenced by the Ag grids. The decrease in the ohmic resistance can be ascribed to the increase of reaction sites, which is caused by the higher electrical conductivity of the Ag grids.¹¹⁾ Along the Ag grids, electrons can be distributed quickly and evenly for

Table 1. Polarization and Ohmic Resistance of Each Sample Measured at 650°C in Ambient Air

Sample	Ohmic resistance ($\Omega \text{ cm}^2$)	Polarization resistance ($\Omega \text{ cm}^2$)
No Ag grid	6.10	1.00
P400	3.55	0.75
P200	3.15	0.60
P100	2.55	0.50

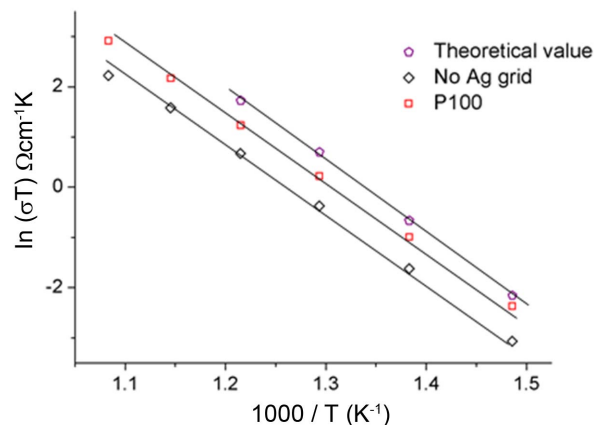


Fig. 5. Arrhenius plot of ohmic ASR of sample with no Ag grids, P100, and theoretical values.

efficient charge transfer reactions between the electrolyte and the electrode, expanding the number of effective reaction sites. Recently, Choi *et al.* reported that the presence of a YSZ-Ag interlayer between the YSZ electrolyte and the LSM-YSZ electrode significantly decreased the ohmic resistance because the high electrical conductivity of Ag reduced the charge transport loss. Our results also show a decrease of the ohmic resistance due to the Ag grids at the electrolyte/electrode interfaces. Moreover, the decrease of the ohmic resistance with the smaller pitch further confirms that the enhanced charge transport due to the Ag grids reduced the ohmic resistance.

Figure 6 shows the imaginary components in the EIS measurements as a function of frequency. The sample with no Ag grids showed a peak frequency of approximately 790 Hz. The specific frequency at which the peak is located represents the rate-limiting step in the electrochemical reactions.¹²⁾ The rate-limiting step in the frequency range of 100–10000 Hz is known to be the charge transfer reactions.¹³⁾ Suppression at this frequency range indicates that the charge transfer reactions were significantly improved due to the presence of the Ag grids because of the catalytic activity of Ag and the fast supply of electrons through the grid structures.^{14–15)} Charge transfer reactions of SOFCs require electrons when dissociated oxygen ions reduce and incorporate into the oxygen vacancies in the electrolyte. Fast delivery of electrons along the Ag grids at the electrolyte/electrode interface may improve the oxygen reduction kinetics, which is known as the most sluggish reaction

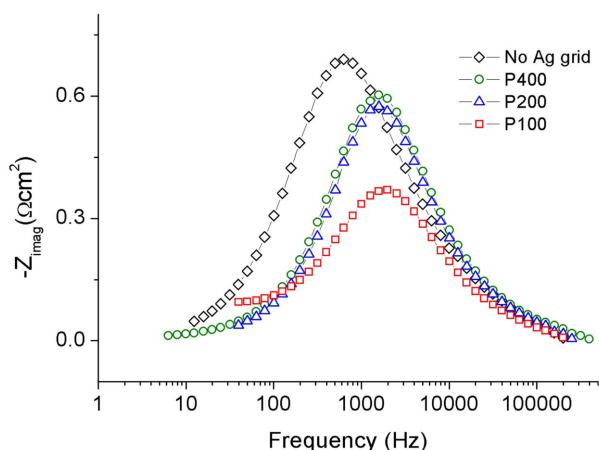


Fig. 6. Bode plot for frequency analysis of no Ag grids (black diamond), P400 (green circle), P200 (blue triangle), and P100 (red square).

step.¹⁶⁾ The smaller magnitude and the smaller pitch substantiates that the active reaction sites at which the charge transfer reaction occur increased with the Ag grids. Therefore, we concluded that the enhanced charge transfer due to the Ag grids reduced the polarization resistance.

It should be noted that, beyond a certain limit, the Ag grids may have an adverse effect on the electrochemical performance. Guo *et al.* reported that the ORR kinetics could be disturbed by excess Ag because of blocking of the active reactions sites at the surface and the interfaces.¹⁷⁻¹⁸⁾ Lee *et al.* also reported that the performance increased with the addition of 3 wt% of Ag, but decreased with the addition of 5 wt% of Ag.¹⁸⁾ Even though the electrochemical performance increased with smaller pitch in our experiments, there should be compensation between the advantages and disadvantages of the Ag grids. As Ag covers more of the YSZ surface with smaller pitches, the number of reaction sites at the electrolyte/electrode interfaces will decrease, reducing the performance. Exploring the optimal geometry of the Ag grids for maximized performance will be a subject of future work.

Our results clearly demonstrate the unique advantages of EHD jet printing. First, this method allows the systematic control necessary to investigate the relationship between the geometry and the electrochemical impedance at micrometer scale. Second, the process is relatively simple and fast, and can be employed to cover large areas for industrial purposes; it is not limited to lab-scale experiments. Therefore, our results may open the possibility of using EHD jet printing to fabricate highly efficient current collectors.

4. Conclusions

We have reported the specific role of Ag grids at the electrolyte/electrode interface for improving the electrochemical performance of SOFCs. To systematically investigate the

geometrical effects of the Ag grids, EHD jet printing was employed. With the Ag grids, both the ohmic and polarization resistances decreased, and higher enhancement was observed when a smaller pitch was utilized. With Ag grids of 100 μm pitch, both the ohmic and polarization resistances decreased by a factor of 2. The effective delivery and distribution of electrons along the Ag grids improved the charge transport and transfer at the electrolyte/electrode interface, extending the number of active reaction sites. Our results demonstrate the possibility of using EHD jet printing for the fabrication of efficient current collectors for SOFCs.

Acknowledgments

This research was supported by the Basic Science Research Program through the National Research Foundation of Korea (NRF), funded by the Ministry of Science, ICT & Future Planning (Grant No. NRF-2013R1A1A1059845).

REFERENCES

1. E. D. Wachsman and K. T. Lee, "Lowering the Temperature of Solid Oxide Fuel Cells," *Science*, **334** [18] 935-39 (2011).
2. J.-W. Son and H. S. Song, "Influence of Current Collector and Cathode Area Discrepancy on Performance Evaluation of Solid Oxide Fuel Cell with Thin-film-processed Cathode," *Int. J. Precis. Eng. Manuf. -Green Techn.*, **1** [4] 313-16 (2014).
3. H. S. Noh, J. Hwang, K. Yoon, B.-K. Kim, H.-W. Lee, J.-H. Lee, and J.-W. Son, "Optimization of Current Collection to Reduce the Lateral Conduction Loss of Thin-film-processed Cathodes," *J. Power Sources*, **230** 109-14 (2013).
4. M. Guillodo, P. Vernoux, and J. Fouletier, "Electrochemical Properties of Ni-YSZ Cermet in Solid Oxide Fuel Cells," *Solid State Ion.*, **127** [1-2] 99-107 (2000).
5. S. P. Jiang, J. G. Love, and L. Apateanu, "Effect of Contact Between Electrode and Current Collector on the Performance of Solid Oxide Fuel Cells," *Solid State Ion.*, **160** [1-2] 15-26 (2003).
6. A. Rolle, V. Thoréton, P. Rozier, E. Capoen, O. Menétré, B. Boukamp, and S. Daviero-Minaud, "Evidence of the Current Collector Effect: Study of the SOFC Cathode Material $\text{Ca}_3\text{Co}_4\text{O}_{9+\delta}$," *Fuel Cells*, **12** [2] 288-301 (2012).
7. S. P. Simmer, M. D. Anderson, I. R. Pederson, and J. W. Stevenson, "Performance Variability of $\text{La}(\text{Sr})\text{FeO}_3$ SOFC Cathode with Pt, Ag, and Au Current Collectors," *J. Electrochem. Soc.*, **152** [9] 1851-59 (2005).
8. M. Casarin and V.M. Sglavo, "Effect of the Current Collector on Performance of Anode-Supported Microtubular Solid Oxide Fuel Cells," *J. Fuel Cell. Sci. Tech.*, **12** 031005-1-6 (2015).
9. S. H. Choi, C. S. Hwang, and M. H. Lee, "Performance Enhancement of Freestanding Micro-SOFCs with Ceramic Electrodes by the Insertion of a YSZ-Ag Interlayer," *ECS Electrochem. Lett.*, **3** [9] 57-59 (2014).
10. Y. Jang, J. Kim, and D. Byun, "Invisible Metal-grid Transparent Electrode Prepared by Electrohydrodynamic (EHD)

- Jet Printing,” *J. Phys. D. Appl. Phys.*, **46** 155103-1-6 (2013).
11. J. G. -Barriocanal, A. R. -Calzada, M. Varela, Z. Sefriouri, E. Iborra, C. Leon, S. J. Pennycook, and J. Santamaria, “Colossal Ionic Conductivity at interfaces of Epitaxial $\text{ZrO}_2\text{:Y}_2\text{O}_3/\text{SrTiO}_3$ Heterostructures,” *Science*, **321** [1] 676-79 (2008).
 12. M. Koyama, C. -Ju. Wen, T. Masuyama, J. Otomo, H. Fukunaga, K. Yamada, K. Eguchi, and H. Takahashi, “The Mechanism of Porous $\text{Sm}_{0.5}\text{Sr}_{0.5}\text{O}_3$ Cathodes Used in Solid Oxide Fuel Cells,” *J. Electrochem. Soc.*, **148** [7] A795-801 (2001).
 13. P. Möller, R. Kanarbik. I. Kivi, and E. Lust, “Influence of Microstructure on the Electrochemical Behavior of LSC Cathodes for Intermediate Temperature SOFC,” *J. Electrochem. Soc.*, **160** [11] 1245-53(2013).
 14. S. Wang, T. Kato, S. Nagata, T. Honda, T. Kaneko, N. Iwashita, and M. Dokiya, “Performance of $\text{La}_{0.6}\text{Sr}_{0.4}\text{Co}_{0.8}\text{Fe}_{0.2}\text{O}_3\text{-Ce}_{0.8}\text{Gd}_{0.2}\text{O}_{1.9}\text{-Ag}$ Cathode for Ceria Electrolyte SOFCs,” *Solid State Ion.*, **146** [3-4] 203-10 (2002).
 15. Y. K. Li, H. J. Choi, H. K. Kim, N. K. Chean, M. Kim, J. Koo, H. J. Jeong, D.Y. Jang, and J. H. Shim, “Nanoporous Silver Cathodes Surface-treated by Atomic Layer Deposition of Y:ZrO_2 for High-Performance Low-temperature Solid Oxide Fuel Cells,” *J. Power Sources*, **295** 175-81 (2015).
 16. L.-P. Sun, H. Zhao, Q. Li, L.-H. Huo, J.-P. Viricelle, and C. Pijolat, “Study of Oxygen Reduction Mechanism on Ag Modified $\text{Sm}_{1.8}\text{Ce}_{0.2}\text{CuO}_4$ Cathode for Solid Oxide Fuel Cell,” *Int. J. Hydrogen Energ.*, **38** [32] 14060-66 (2013).
 17. W. Zhou, R. Ran, Z. Shoa, R. Cai, W. Jin, N. Xu, and J. Ahn, “Electrochemical Performance of Silver-modified $\text{Ba}_{0.5}\text{Sr}_{0.5}\text{Co}_{0.8}\text{Fe}_{0.2}\text{O}_{3.5}$ Cathodes Prepared via Electroless Deposition,” *Electrochim Acta*, **53** [13] 4370-80 (2008).
 18. K. T. Lee and A. Manthiram, “Electrochemical Performance of $\text{Nd}_{0.6}\text{Sr}_{0.4}\text{Co}_{0.5}\text{Fe}_{0.5}\text{O}_{3.6}\text{-Ag}$ Composite Cathodes in Intermediate Temperature Solid Oxide Fuel Cells,” *J. Power Sources*, **160** [2] 903-8 (2006).